



UNITED NATIONS
Office for Outer Space Affairs



**United Nations International Conference on Space-based Technologies for
Disaster Risk Reduction - "Building Resilience through Integrated Applications"**

Impacts of different sources of topographic data and uncertainty assessment on 1-D 2-D coupled flood inundation modelling

Mohit Prakash Mohanty, Nithya S, J. Indu, Subimal Ghosh and Subhankar Karmakar

Presented by

Mohit Prakash Mohanty

Centre for Environmental Science and Engineering

INDIAN INSTITUTE OF TECHNOLOGY BOMBAY

Powai, Mumbai 400 076

24 October 2017

Outline of presentation

- a) Introduction
- b) Literature review
- c) Objectives of the research
- d) Proposed framework
- e) Description of the study area
- f) Data and methodology
- g) Major findings
- h) Concluding remarks

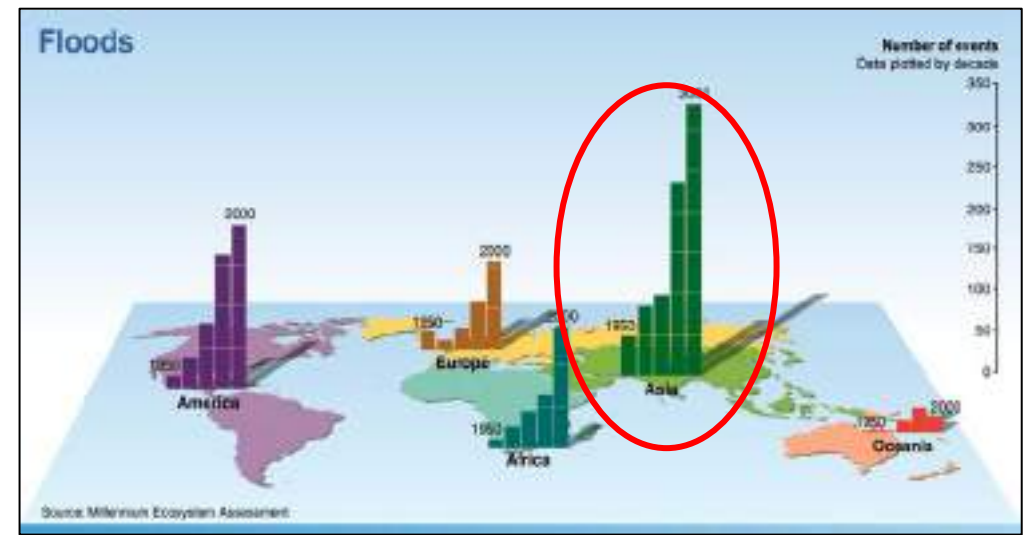
Introduction

Flood : Overflow of water that submerges land which is usually dry [The European Union (EU) Flood directive].

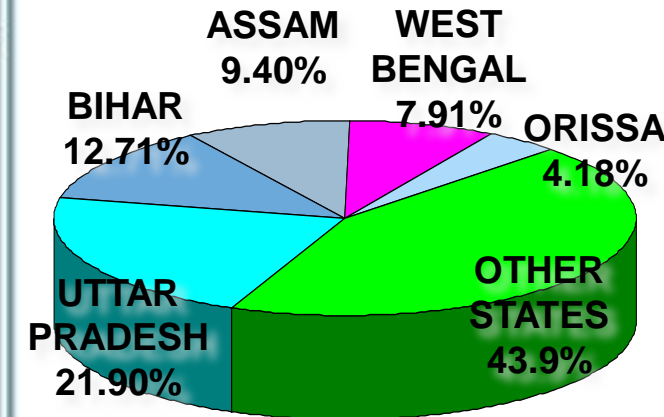
Flood situation in the Indian sub-continent

- ❖ 1/8th of the total geographical area, which sums up to 40 million hectares is flood prone (Singh and Prokop, 2015)
- ❖ 4.84 million people are affected annually by riverine floods each year, taking the economic damage to as high as 36,004.75 million INR (Central Water Commission, 2010).
- ❖ Major contributing factors: ineffectiveness in proper flood risk management added with the impacts of climate change and unplanned socio-economic development (Basha and Rus, 2004)

The risk to riverine flooding is increasingly serious in India, majorly contributed by the monsoon rainfall from June to September, triggered with tidal disturbances along the long coastline (NDMA 2008).

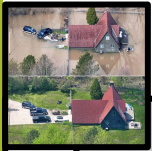


Source: Millennium Ecosystem assessment (<https://www.grida.no/resources/6062>)



Source: National Disasters Association (<http://www.n-d-a.org/>)

Impacts and major drivers of Riverine Floods



Long term impacts

- Rebuilding of roads and infrastructure
- Uninsured losses, Loss of trade and industry
- Costs of insurance



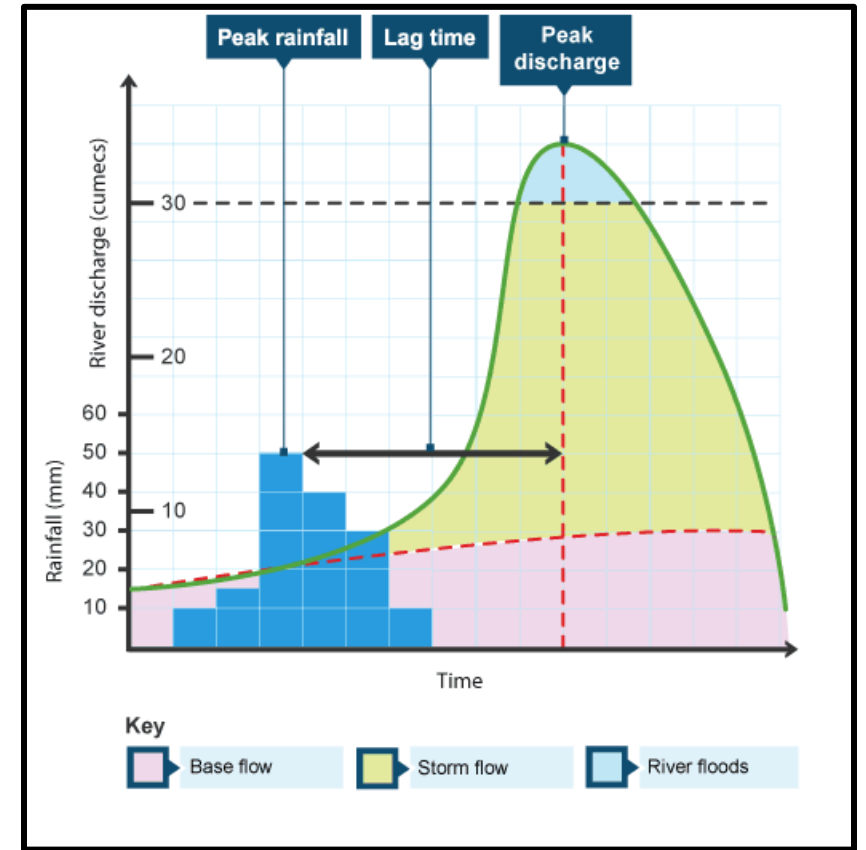
Short term impacts

- Death, Injury
- Loss of Infrastructure
- Damage to Property and Business
- Disease/ Epidemics

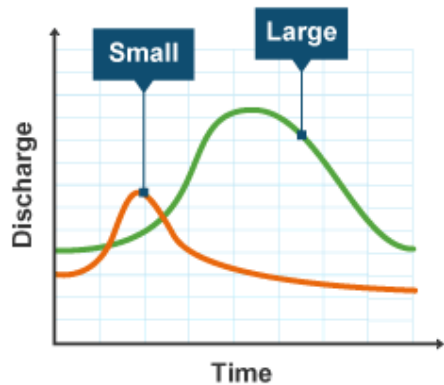


Intangible impacts

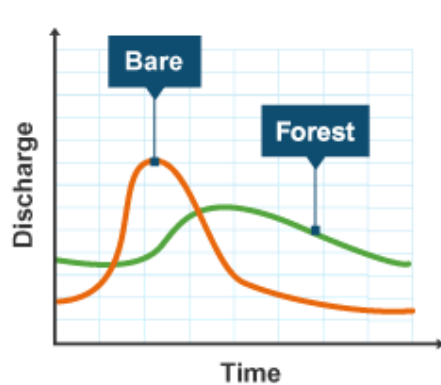
- Emotional and Psychological damage
- Sentimental loss of property or items
- Sleeplessness, Irritability or tiredness, Depression



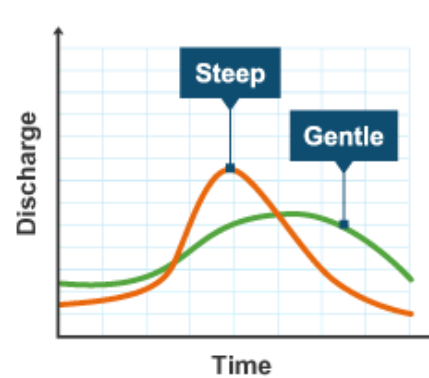
Size of drainage basin



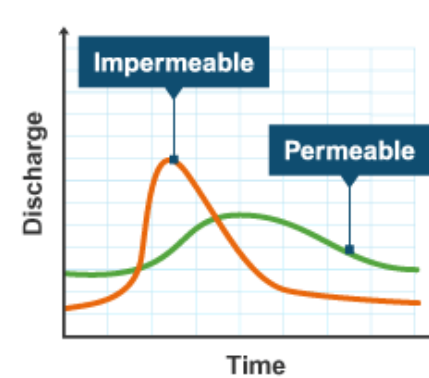
Vegetation



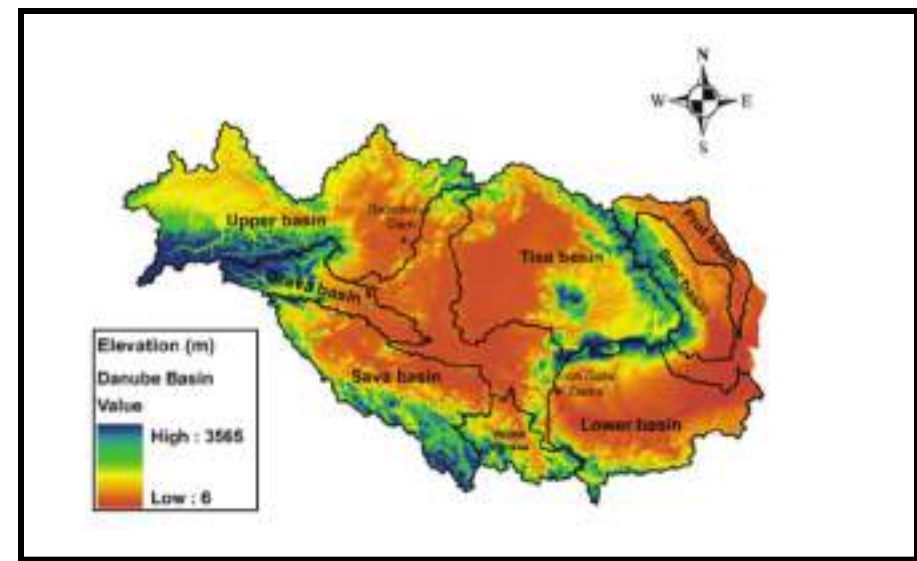
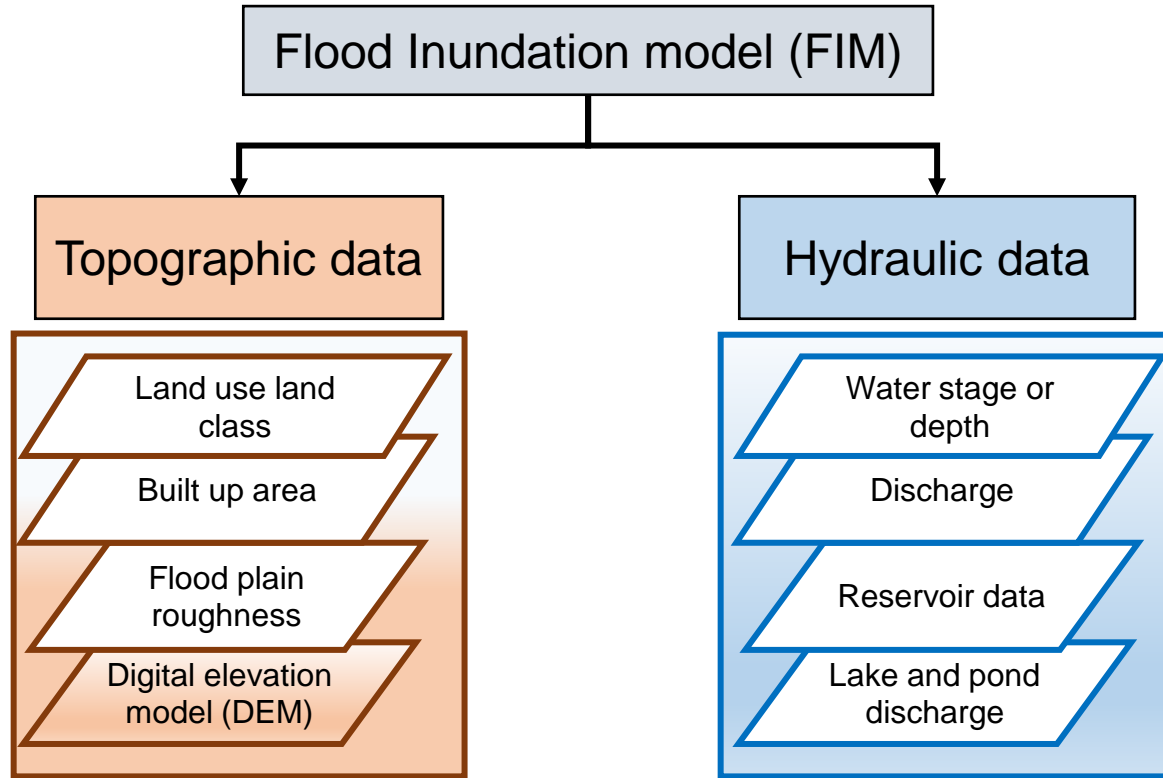
Valley side steepness



Soil type



Description of hydrodynamic flood modelling



- ❖ Raster data (evenly spaced, gridded data)
- ❖ Cells hold values for the height of a feature or site referenced to a common vertical datum
- ❖ Resolution refers to the size of the pixels in the data
Ex:-A DEM with 30 meter resolution is composed of all cells being 30 meters x 30 meters in the x and y directions and each cell holds a single elevation value (z)

GLOBAL SOURCES OF DEMs

- ❖ SRTM and ASTER global DEM from United States Geological Survey (USGS)
- ❖ JAXA's Global ALOS 3DWorld
- ❖ WORLD DEM
- ❖ AW3D Inter Map

NATIONAL SOURCES OF DEMs

- ❖ National Elevation Dataset and GTOPO30 for USA
- ❖ CARTO DEM product for India
- ❖ Canadian DEM (CDEM) for Canada
- ❖ EU-DEM for entire Europe
- ❖ AHN-2 for the Netherlands
- ❖ NZ 8m DEM

Overview of various DEMs considered

LiDAR DEM

- LiDAR (**L**ight **D**etection **A**nd **R**anging) uses an active sensor in air borne instrument to emit energy (light) and detect returned energy
- Data can be collected in day or at night
- Combines GPS and an Inertial Measurement device to compute x,y,z positions.
- **Grid resolution: usually very high (< 5 metres)**

CARTO DEM

- Carto DEM is generated using Augmented Stereo Strip Triangulation (ASST) - indigenously developed software by Space Application Centre, ISRO (India).
- The generated DEM and ortho images of each Cartosat-1 segment are cut into tiles of 7.5'x7.5' extents.
- The entire Indian region is covered by approximately 500 Cartosat-1 segments with a total number of around 20,000 tile pairs.
- **Grid resolution: 2.5, 10, and 30 m**

SRTM DEM

- The NASA Shuttle Radar Topographic Mission (SRTM) has provided digital elevation data (DEMs) for over 80% of the globe.
- This data is currently distributed free of charge by USGS and is available for download from the National Map Seamless Data Distribution System, or the USGS ftp site.
- **Grid resolution: 30 and 90 m**

ASTER DEM

- The ASTER Global Digital Elevation Model (ASTER GDEM) is a joint product developed and made available to the public by the Ministry of Economy, Trade, and Industry (METI) of Japan and the United States National Aeronautics and Space Administration (NASA).
- It is generated from data collected from the Advanced Spaceborne Thermal Emission and Reflection Radiometer (ASTER), a spaceborne earth observing optical instrument.
- **Grid resolution: 30 m**

Literature review

Effect of different sources of topography on flood inundation modeling

DEMs used	Major findings	Reference
<ul style="list-style-type: none">• European Remote Sensing (ERS) satellite data• Contour data• Contour data supplemented with DGPS	<ul style="list-style-type: none">• Significant differences in the spatial extent of flood with the usage of these DEMs	Wilson and Atkinson (2005)
<ul style="list-style-type: none">• Laser altimetry• GPS survey• vectorial cartography	<ul style="list-style-type: none">• GPS-based DEM gave the best performance in simulating the water level and flood inundation area• Contour-based data showed the largest discrepancies	Casas et al. (2006)
<ul style="list-style-type: none">• LiDAR DEM• SRTM• NED• Interferometric Synthetic Aperture Radar (IfSAR)	<ul style="list-style-type: none">• Usage of LiDAR DEM could provide better flood inundation depths and extent, followed by IfSAR, SRTM and NED DEM	Sanders (2007)
<ul style="list-style-type: none">• LiDAR• Topographic contours• SRTM	<ul style="list-style-type: none">• LiDAR utilised flood simulations showed the lowest error, followed by the contour and SRTM DEM	Schumann et al. (2008)
<ul style="list-style-type: none">• NED• LiDAR	<ul style="list-style-type: none">• Coarser grid size contributed to higher values of water levels and hence larger flood inundation extents	Cook and Merwade (2009)
<ul style="list-style-type: none">• GPS• Photogrammetric• Terrestrial laser scanning point data sets	<ul style="list-style-type: none">• Improved accuracies and inundation prediction using GPS-derived DEMs	Coveney and Fotheringham (2011)
<ul style="list-style-type: none">• SRTM• HYDRO1K DEMs	<ul style="list-style-type: none">• The SRTM DEM showed less vertical error compared to the other DEM, and hence was found to be more suitable than the other DEM in flood modelling	Karlsson and Arnberg (2011)

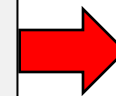
Literature review

Effect of DEM grid size and resampling on flood Modeling

DEMs used	Major findings	Reference
<ul style="list-style-type: none">Spot elevation data resampled to grid resolutions of 2, 4, 10, 30, and 90 m	Resolutions up to 10 m displayed improved modeling results	Zhang and Montgomery (1994)
<ul style="list-style-type: none">LiDAR derived DEM (2.5 m) data resampled to grid resolutions of 5, 10, and 25 m	The spatial extent of flood inundation increased as the grid resolution became coarser	Werner (2001)
<ul style="list-style-type: none">LiDAR derived DEM at a resolution of 10 m(original) and resampled to 20, 50, 100, 250, 500 and 1000 m.	Optimum resolution of 100 m could provide a better flood inundation output when validated with the observed satellite observations	Horritt and Bates (2001)
<ul style="list-style-type: none">Original DEM (1 m) resampled to lower resolutions (10, 50 and 100 m)	Simulated flood inundation extent decreased while rasterizing the original DEM (1 m) to lower resolutions (10, 50 and 100 m)	Brandt (2005)
<ul style="list-style-type: none">Original 6 m and 3 m LiDAR DEM resampled to grid sizes ranging from 9 m to 100 m, and 6 m to 100 m respectively	Linear relationship of the water level and flood inundation area with the increase in grid size.	Saksena and Merwade (2015)

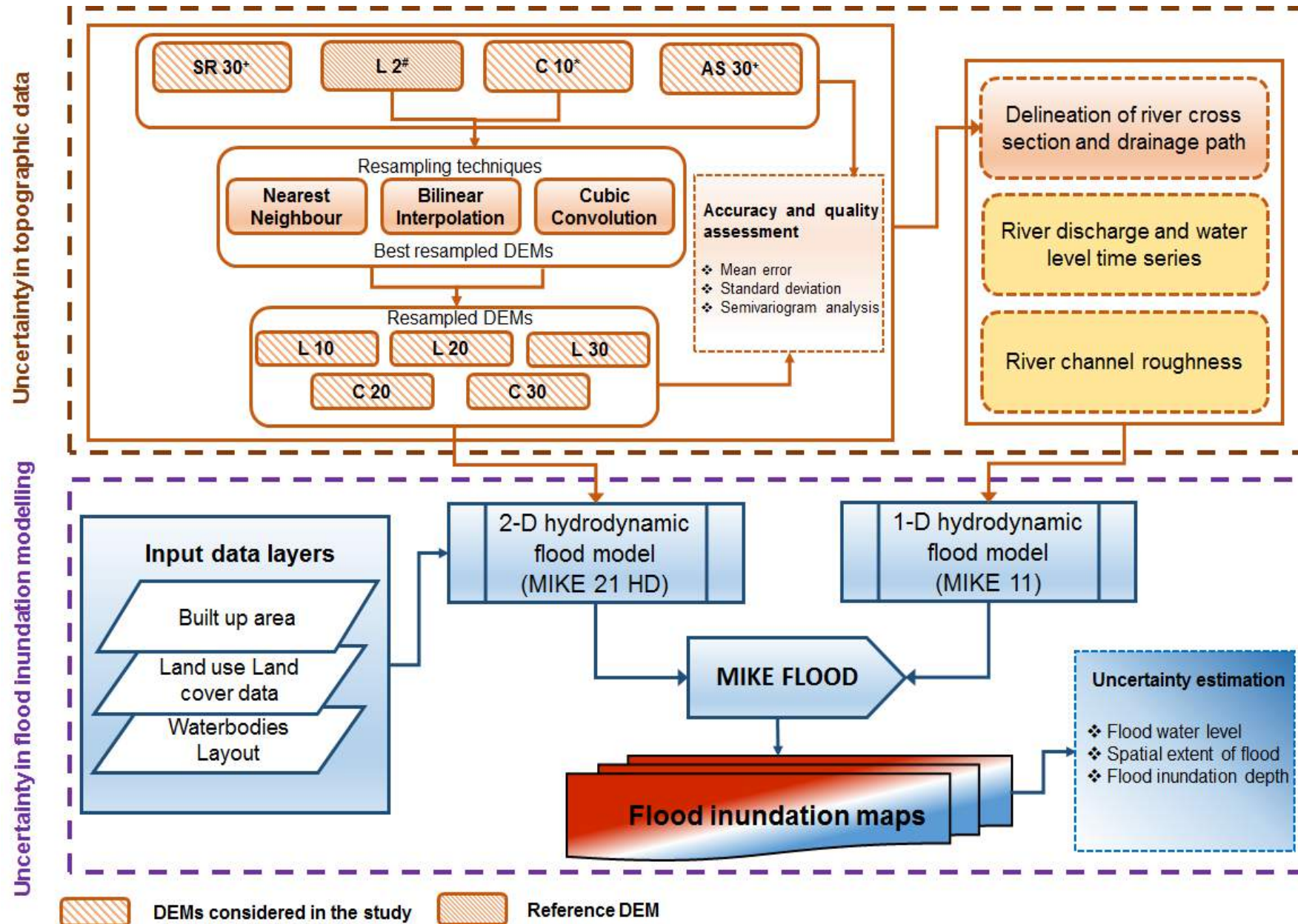
Major research questions

- How does the uncertainty in water level and flood inundation depth change with different types of DEMs ?
- What is the level of uncertainty associated with 1-D, 2-D and 1-D 2-D coupled flood inundation modelling?
- How does grid resolution of a DEM affect the inundation extent and depth?



- ❖ Geo-statistical analysis of various DEMs in terms of quality and accuracy assessment
- ❖ Uncertainty in water level, flood inundation extent and depth using 1-D 2-D coupled inundation modeling

Proposed framework



Commercially available DEMs, *Nation wide available DEMs, +Globally available DEMs

Description of study area

Jagatsinghpur district: A challenge to modelling extreme events

- Jagatsinghpur district (geographical area: 1760 km²): regarded as highly flood prone, cyclone prone and drought prone area in Odisha.
- Lies in the lower Mahanadi basin and falls within two deltaic zones: the Mahanadi and the Devi and the other side is surrounded by the Bay of Bengal.
- Between 2001 to 2008: **76751 people** (approximate 126 villages) were affected, **1130 hectares cropped area** were damaged due to flooding only in Jagatsinghpur block.



Location of Jagatsinghpur district

Source: Jagatsinghpur district website (jagatsinghpur.nic.in/)

Description of study area

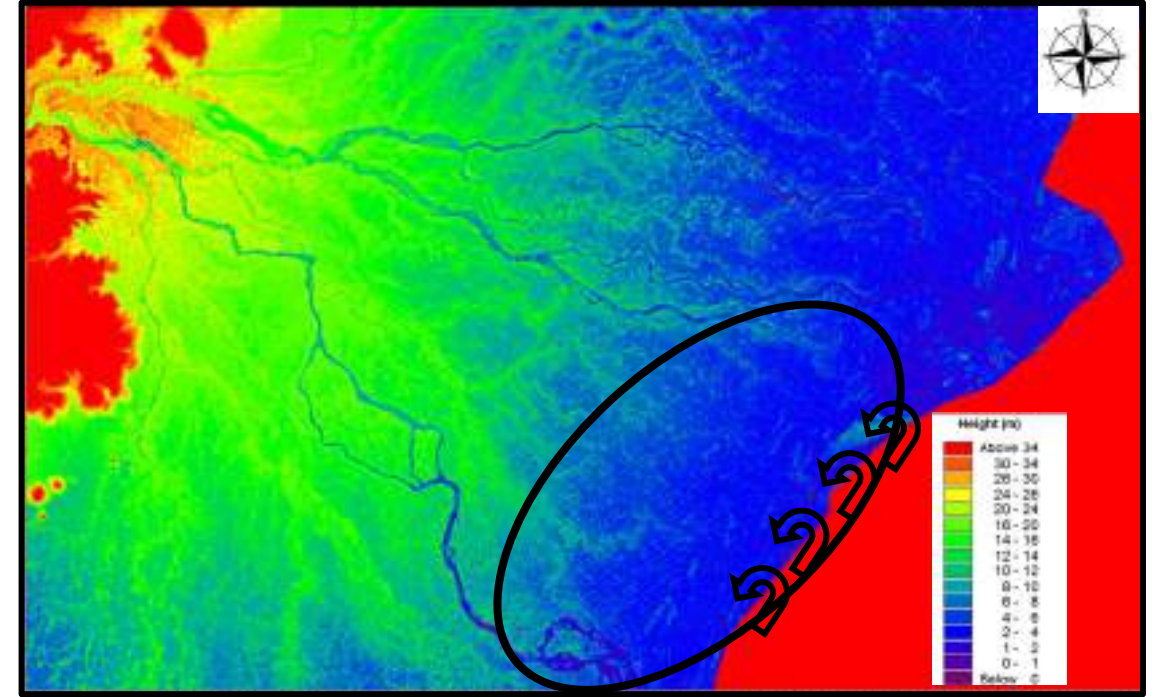
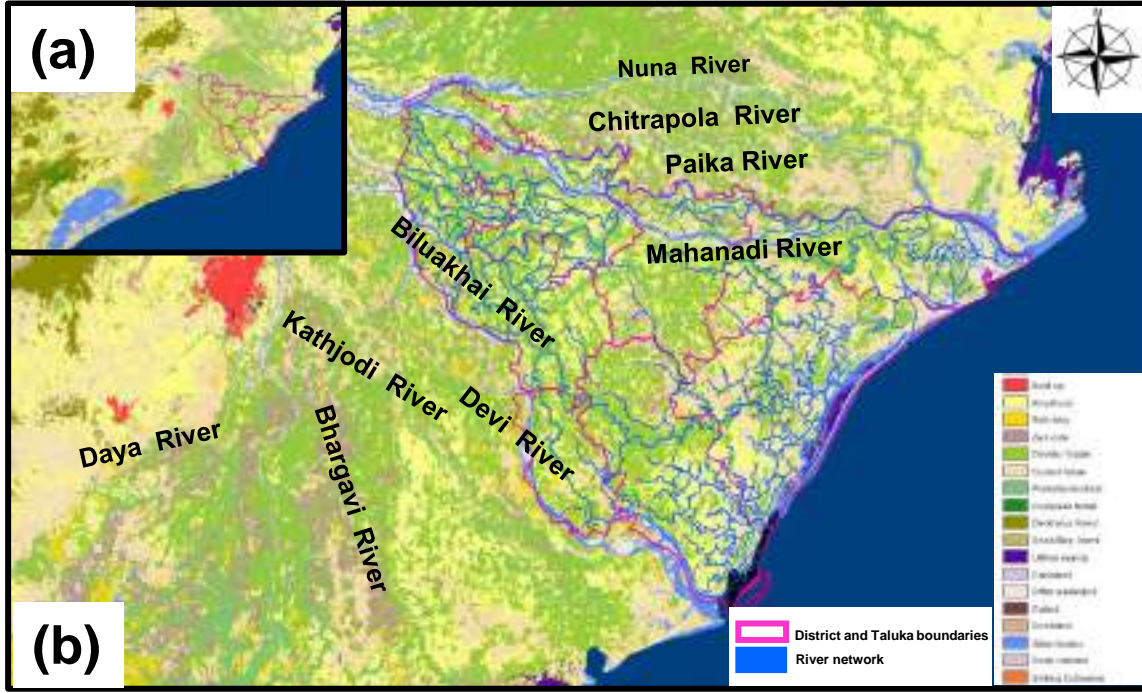
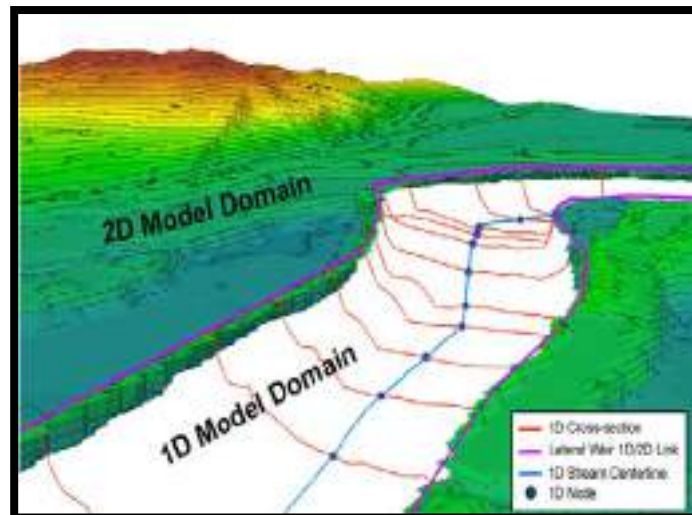


Figure. Description of the study area: (a) The inset map shows the location of Jagatsinghpur district in the lower Mahanadi basin; bounding box represents the area considered for flood modelling; (b) The study area with various land use classes and major rivers contributing to flood (c) Bathymetry (DEM) of the study area.

$$\frac{\partial Q}{\partial t} + \frac{\partial(\alpha \frac{Q^2}{A})}{\partial x} + gA \frac{\partial h}{\partial x} + \frac{gQ|Q|}{C^2AR} = 0$$



$$\frac{\partial \zeta}{\partial t} + \frac{\partial p}{\partial x} + \frac{\partial Q}{\partial y} = \frac{\partial d}{\partial t}$$

$$\frac{\partial}{\partial y} \left(\frac{pq}{H} \right) + gh \frac{\partial \zeta}{\partial x} + \frac{gp\sqrt{p^2+q^2}}{c^2H^2} - \frac{1}{\rho_w} \left[\frac{\partial}{\partial x} (H_{xx}) + \frac{\partial}{\partial y} (H_{xy}) \right] - \Omega_q - fV_{xx} + \frac{h\partial}{\rho_w \partial x} (p_a) = 0$$

Q is discharge (m³/s), A is the cross-sectional area (m²), q is the lateral inflow (m³/s/m), h is the stage above datum (m), C is the Chezy's roughness coefficient (m^{1/2}/s), R is the hydraulic radius (m), α is the momentum distribution coefficient (s²/m³), g is the gravitational acceleration (m/s²), x and t are the distance (m) and time (s) respectively

where ζ is the surface elevation (m), t is time (sec), p is flux density in x direction (m³/s/m), x, y are space coordinates, d is time-varying water depth (m), h is water depth (m), g is acceleration due to gravity (m/s²), C is Chezy resistance coefficient (m^{1/2}/s), Ω_q is Coriolis parameter (s⁻¹), and ρ_w is density of water and f(V) is wind friction factor.

Data and methodology

Various DEMs used in the study

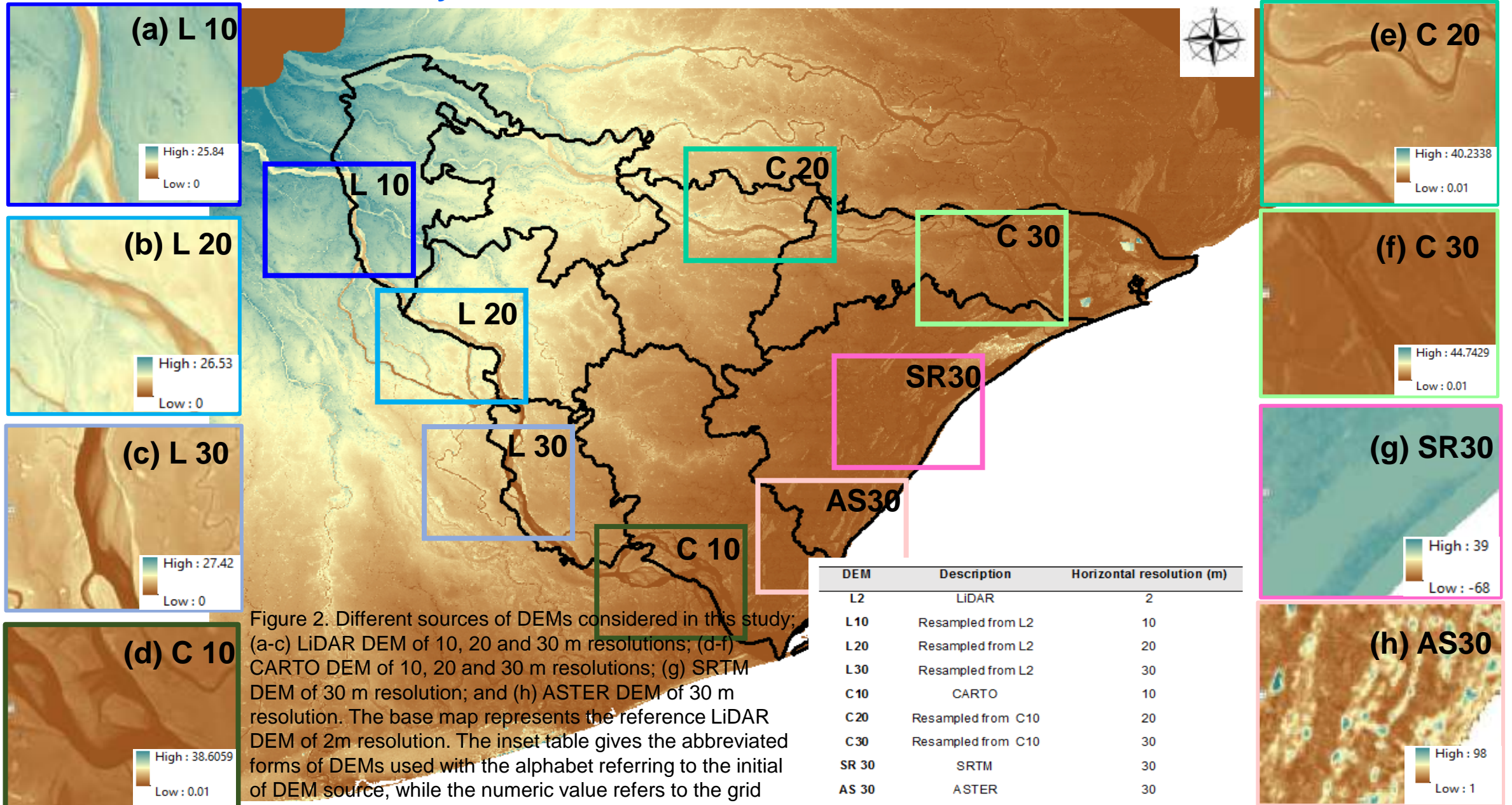


Figure 2. Different sources of DEMs considered in this study; (a-c) LiDAR DEM of 10, 20 and 30 m resolutions; (d-f) CARTO DEM of 10, 20 and 30 m resolutions; (g) SRTM DEM of 30 m resolution; and (h) ASTER DEM of 30 m resolution. The base map represents the reference LiDAR DEM of 2m resolution. The inset table gives the abbreviated forms of DEMs used with the alphabet referring to the initial of DEM source, while the numeric value refers to the grid resolution.

Data and methodology



Figure. Location of 1832 settlement (control) points located in the study area for extraction of vertical heights in different sets of DEMs.

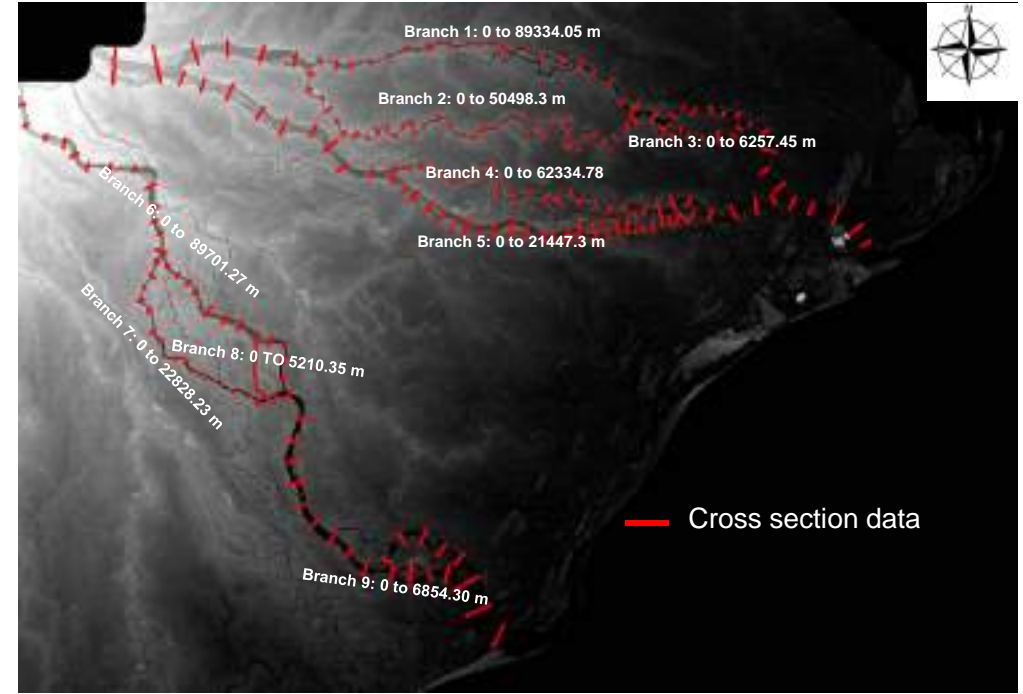


Figure. Extraction of cross section data at various stretches of different rivers in Jagatsinghpur district (The lengths of different streams are mentioned in brackets).

$$\text{Mean Error (ME)} = \frac{\sum_{i=1}^n (E_{L2_i} - E_{DEM_i})}{n}$$

$$\text{Standard Deviation (STD)} = \sqrt{\frac{\sum_{i=1}^n [(E_{L2_i} - E_{DEM_i}) - \text{ME}]^2}{n}}$$

$$\text{LE90} = 1.65(\text{STD})$$

where, E_{L2} represents the elevation value for the reference DEM i.e. LiDAR 2m (L2) at the i^{th} point; E_{DEM_i} represents the elevation value for different DEMs at the i^{th} point, and n corresponds to the number of control points under consideration.

Data and methodology

Table. Details of hydraulic and meteorological inputs used in the study

Data	Description	Purpose of use	Source
Discharge	Daily discharge data (m ³ /s) for 2011 flood event	MIKE 11 model (as upstream boundary condition)	Central Water Commission, India
Water level	Daily water level data (m) for 2011 flood event	MIKE 11 model (for calibration)	Central Water Commission, India
Tidal data	Daily tidal height (m)	MIKE 21 model input (as downstream boundary condition)	INCOIS, Hyderabad
Rainfall	Daily block-wise rainfall data for 2011 flood event	MIKE 21 model input (as boundary condition)	State water resources department, Odisha (India): http://www.odisha.gov.in/disaster/src/RAINFALL/RAINFALL10/RAINFALL.html
LU-LC data	Land use Land cover data	MIKE 21 model input (as resistance values)	National Remote Sensing Centre, Hyderabad

Major findings which may be worth sharing

Geo-statistical analysis of various DEMs

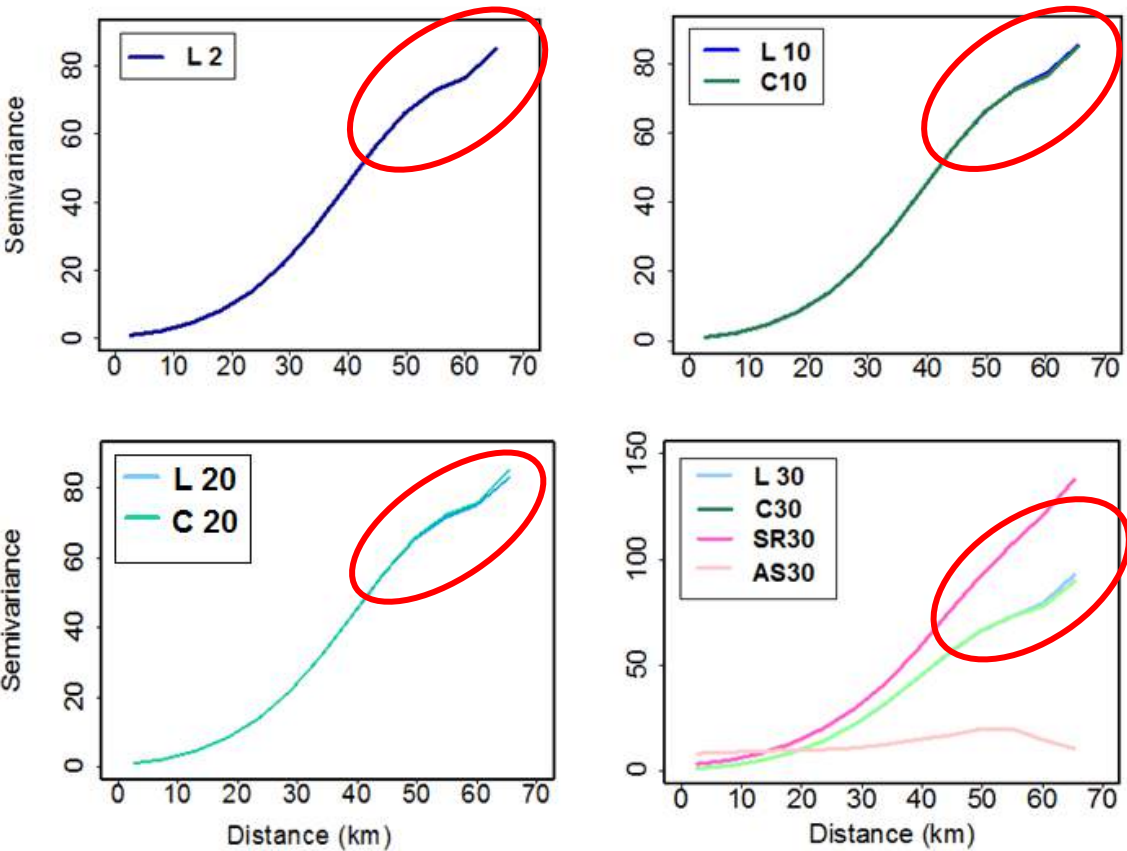


Figure. Omnidirectional semivariogram plots for (a) LiDAR 2m; (b) LiDAR and CARTO (10m); (c) LiDAR and CARTO (20m); (d) LiDAR, CARTO, SRTM and ASTER (30 m).

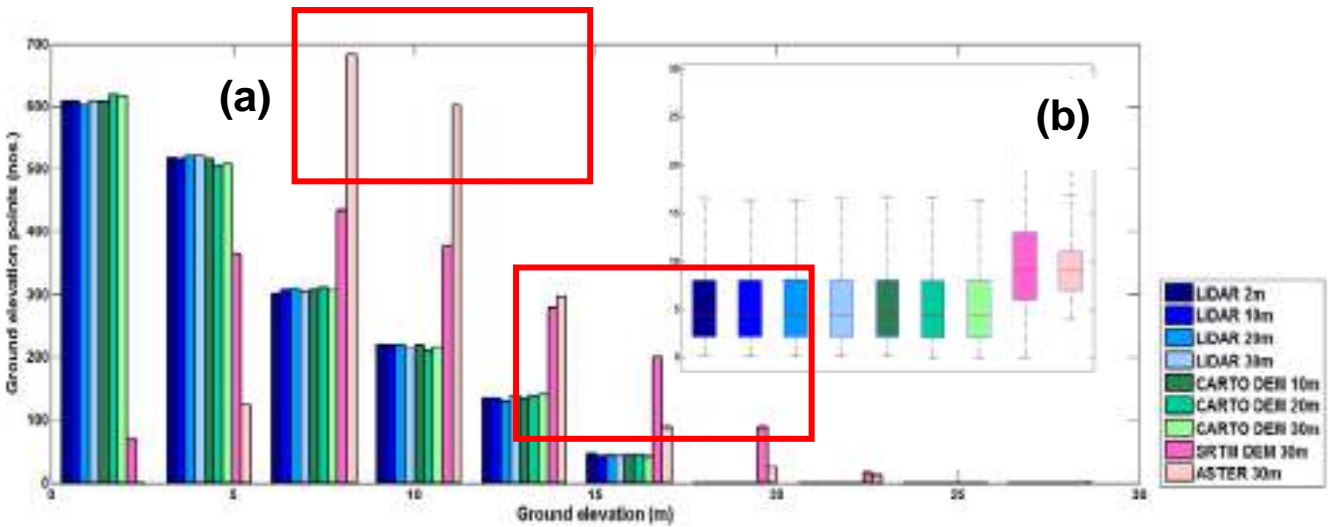


Figure. Histogram plot of the difference in elevations of the ground control points; (b) inset map shows the box plot of elevation captured for different DEMs

Geo-statistical analysis of various DEMs

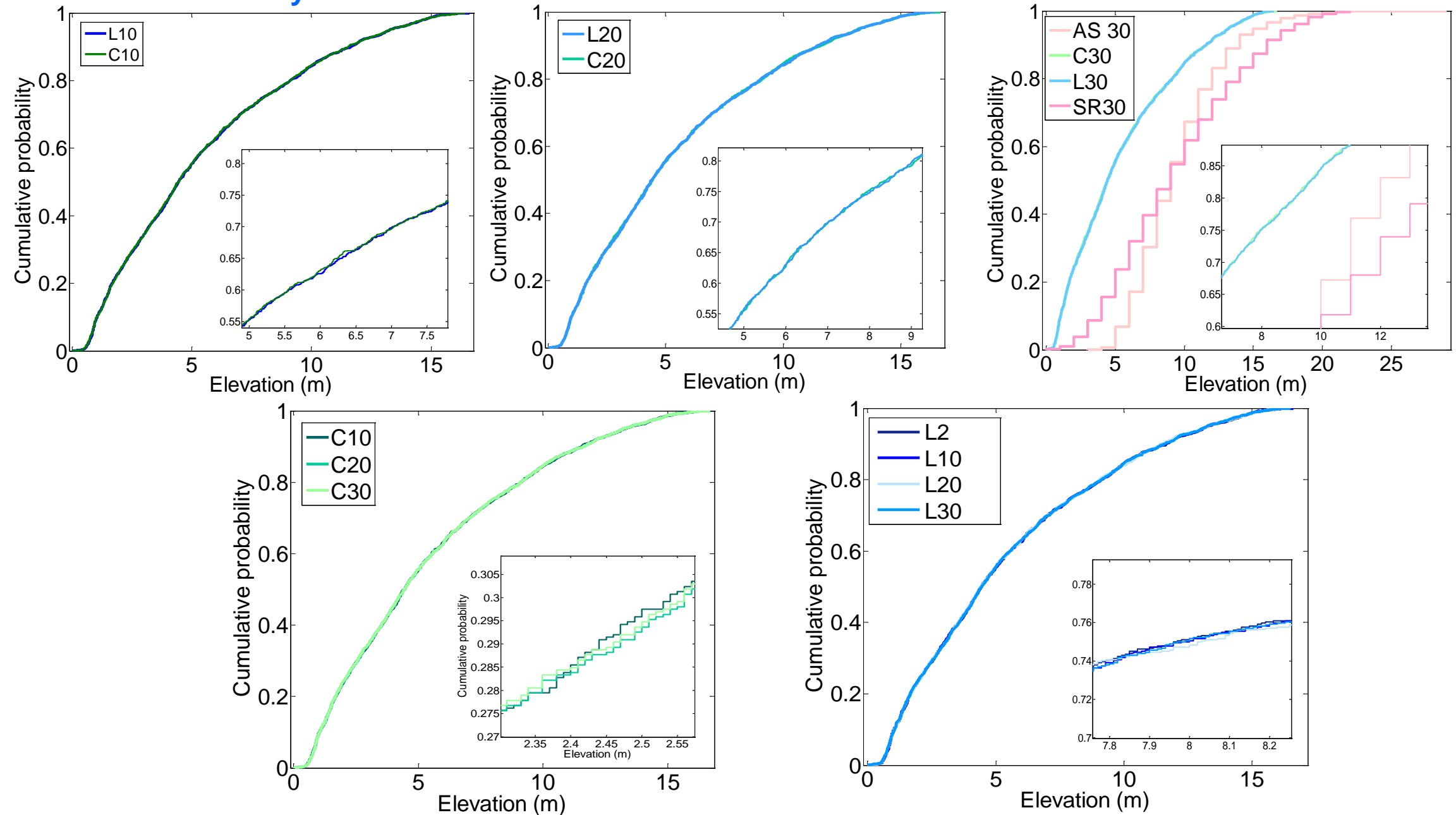


Figure. Comparison of CDF plots between different sources of DEMs (a) L 10 and C10 (b) L20 and C20 (c) L30, C30, SR30 and C30; and resampled DEMs (d) C10, C20 and C30 and (e) L2, L10 L20 and L30

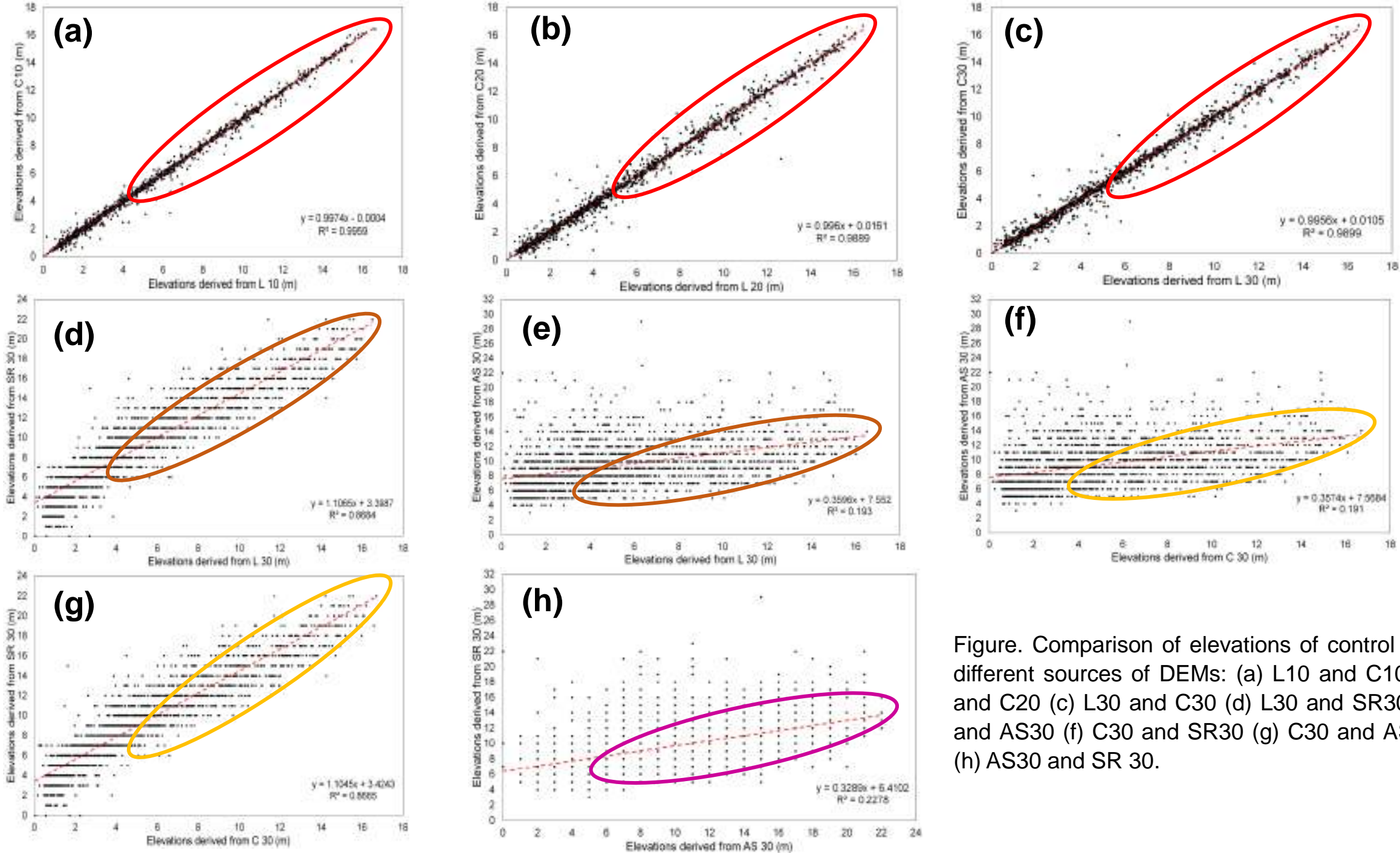


Figure. Comparison of elevations of control points in different sources of DEMs: (a) L10 and C10 (b) L20 and C20 (c) L30 and C30 (d) L30 and SR30 (e) L30 and AS30 (f) C30 and SR30 (g) C30 and AS30 and, (h) AS30 and SR 30.

Major findings which may be worth sharing

Uncertainty in channel water depth through 1-D modelling

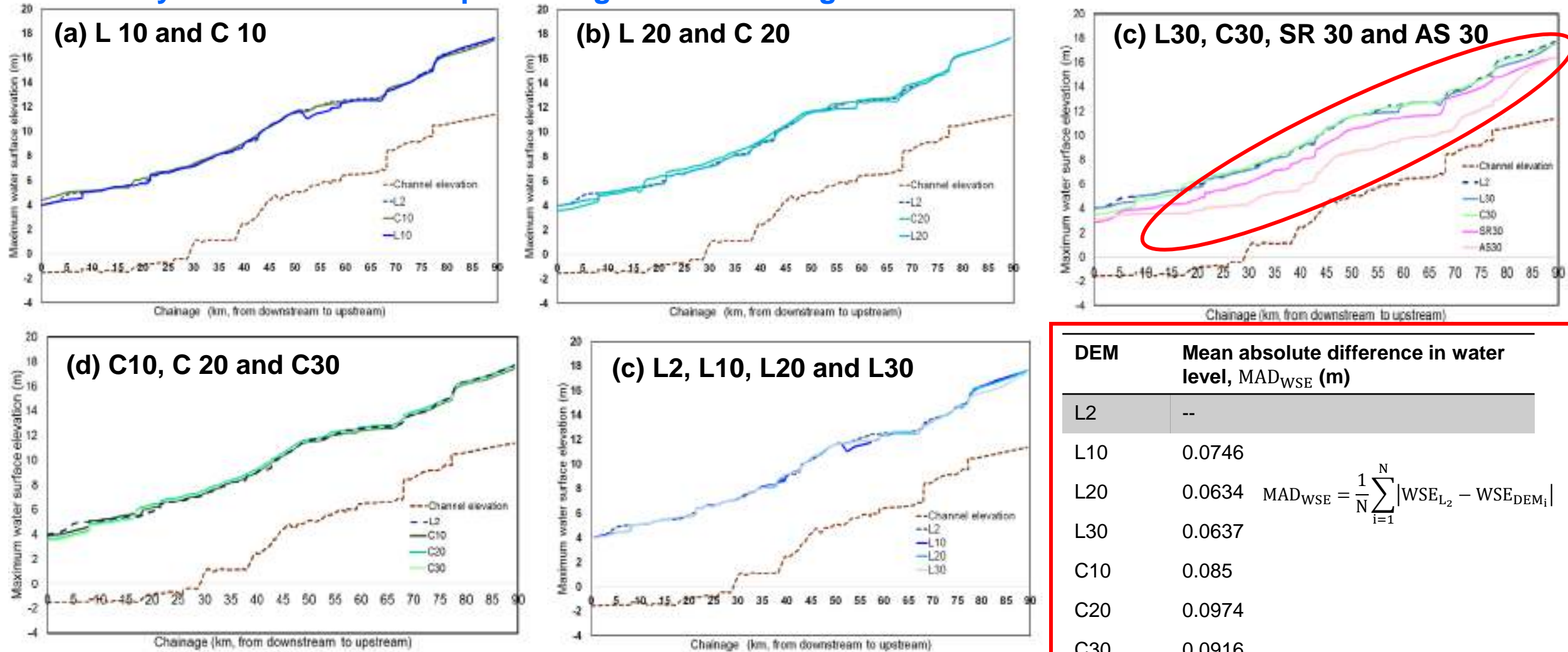


Figure 9. Uncertainty in terms of maximum water level (m) simulated for the 2011 flood event along branch 8 for different sources of DEMs (a) L 10 and C10 (b) L20 and C20 (c) L30, C30, SR30 and AS30 and resampled DEMs (a) C10, C20 and C30 (e) L2, L10, L20 and L30.

DEM	Mean absolute difference in water level, MAD_{WSE} (m)
L2	--
L10	0.0746
L20	0.0634
L30	0.0637
C10	0.085
C20	0.0974
C30	0.0916
SR30	1.016
AS30	2.465

$$MAD_{WSE} = \frac{1}{N} \sum_{i=1}^N |WSE_{L2} - WSE_{DEM_i}|$$

Where, MAD_{WSE} is the mean absolute difference in water depth that is simulated by LiDAR 2m DEM (taken as reference), WSE_{DEM_i} is the water depth simulated by corresponding DEMs, N denotes the number of cross sections where results are compared.

Uncertainty in flood inundation extent through 1-D 2-D coupled modelling

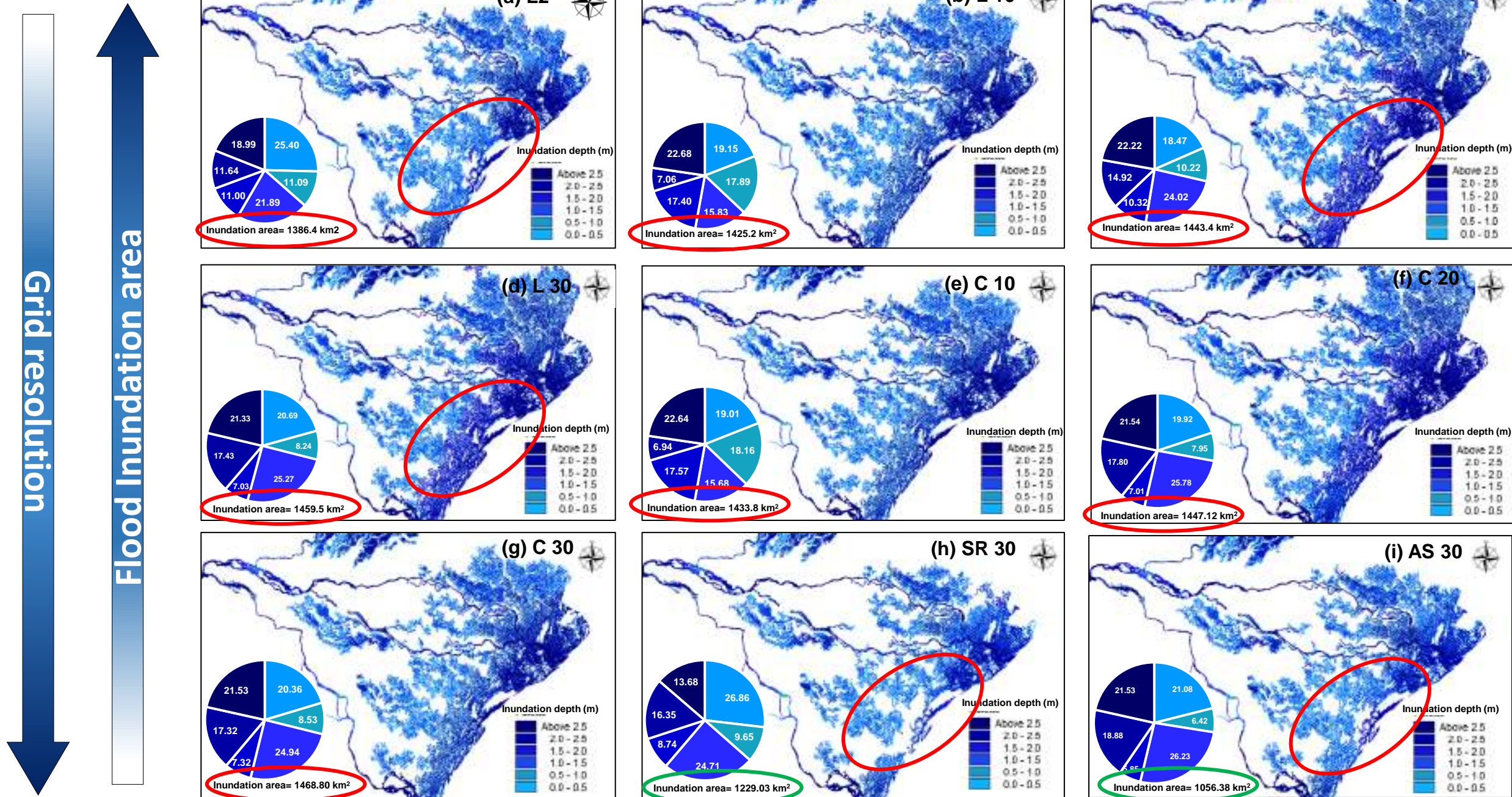


Figure. Uncertainty in spatial extent of flood simulated by 1-D 2-D coupled MIKE FLOOD model for different sets of DEMs (a) L2 (b) L10 (c) L20 (d) L30 (e) C10 (f) C20 (g) C30 (h) SR30 (i) AS30.

Major findings which may be worth sharing

Uncertainty in flood inundation depth through 1-D 2-D coupled modelling

Table. Error statistics of spatial extent of flood for different original and resampled DEMs

DEM	Inundation area (km ²)	Area difference (%)	F* (%)	F(%) ⁺
L2	1386.4		---	---
L10	1425.2	2.78	96.8	---
L20	1443.4	4.11	93.3	---
L30	1459.5	5.27	91.2	---
C10	1433.8	3.41	95.7	97.2
C20	1447.12	4.37	92.6	96.7
C30	1468.80	5.94	90.4	95.4
SR30	1229.03	-11.35	71.8	78.5
AS30	1056.38	-23.8	56.4	60.4

*F(%)⁺ is the measure of fit (%) with those from LiDAR of same resolution (L10, L20 and L30)

$$F(\%) = \frac{A_{L_2} \cap A_{DEM_i}}{A_{L_2} \cup A_{DEM_i}}$$

Where, F (%) is the measure of fit, A_{L_2} is the inundation area from the simulated outputs of the LiDAR 2m reference DEM, A_{DEM_i} is the inundation area from the simulated outputs of other DEMs, \cap and \cup are the intersection and union operations in GIS.

Major findings which may be worth sharing

Uncertainty in flood inundation depth through 1-D 2-D coupled modelling

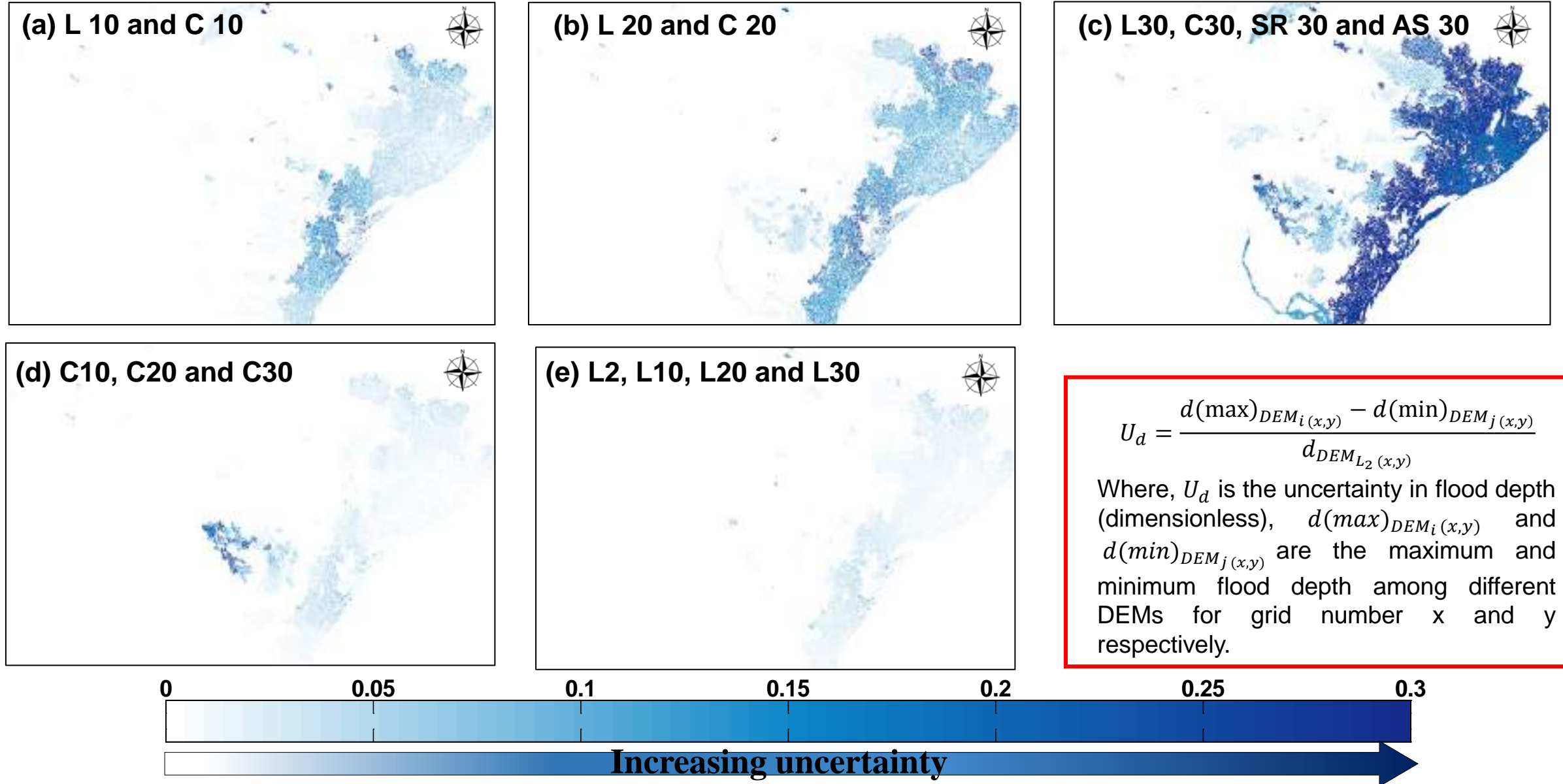


Figure. Uncertainty in inundation depths resulting from various sources of DEMs (a) L10 and C10 (b) L20 and C20 (c) L30, C30, SR30 and AS30 and resampled ones (d) C10, C20 and C30 and (e) L2, L10, L20 and L30.

Concluding remarks

- The study presented here described an important outcome, that the nature of any topographical data needs due consideration before they can be used in flood modelling, particularly for coastal flood risk assessments.
- In particular, the quality and accuracy holds a higher weightage as seen by the performance measures of resampled versions of LiDAR and CARTO DEMs in comparison to SRTM and ASTER.
- This puts forth a key statement of careful selection of these data in flood models after further improvement in the terrain characteristics of the globally and freely available DEMs.
- While the outcome of this work focusses more on the hydrodynamic perspectives, similar study can be carried forward to other modelling aspects as well, such as land surface models.
- As it is well known that a discrepancy in the estimation in flood inundation can affect the management plan and risk thereof for any region, it is necessary to ascertain the quality and source of topographic inputs is given due consideration.

Acknowledgements

- The United Nations Office for Outer Space Affairs (UNOOSA)
- Ministry of Civil Affairs of the People's Republic of China
- National Remote Sensing Centre, Hyderabad (India)
- Central Water Commission, Bhubaneswar; Mahanadi and Eastern Rivers Organisation, Bhubaneswar, Odisha
- Department of Water Resources, Govt. of Odisha (India)
- IIT Bombay (India)

Thank you

mohit2012.env@gmail.com, skarmakar@iitb.ac.in